Supporting Information

Arango et al. 10.1073/pnas.1303726110

SI Materials and Methods

Preparation of Apigenin-Immobilized Polyethyleneglycol-Polyacrylamide Beads. Apigenin was immobilized to amino polyethyleneglycol-polyacrylamide copolymer beads (PEGA beads; EMD Biosciences). Briefly, 0.40 mmol/mg PEGA beads were washed three times with pyridine and subsequently mixed with 3.3 mol equivalents (to the amino group loaded on the beads) of 4-nitrophenyl bromoacetate. Beads were stirred at room temperature for 3 h, filtered, washed three times with ∼10 mL each dichloromethane (CH_2Cl_2), MeOH, and *N*,*N*′-dimethylformamide, and subsequently mixed with 2.2 mol equivalents apigenin and 1.8 mol equivalents K_2CO_3 to the bromoacetyl group loaded on the beads. The resulting suspension was stirred at room temperature for 3 d, filtered, and washed three times with ∼10 mL each CH_2Cl_2, MeOH, and H_2O. The apigenin-immobilized PEGA beads were vacuum-dried. Filtrates were neutralized by the addition of 1 M aqueous HCl. After layer separation, the aqueous layer was extracted seven times with 50 mL EtOAc. The combined organic layer was washed with brine, dried over anhydrous sodium sulfate (Na_2SO_4), and concentrated in vacuo. The unloaded apigenin was recovered from the supernatant by silica gel chromatography (chloroform/MeOH = 20:1). The amount of apigenin immobilized on 1 mg dried PEGA beads was estimated to be ∼0.14 μmol as determined by subtracting the amount of unloaded apigenin from the amount of apigenin used in the reaction.

Plasmid Construction. pEGFP–heterogeneous nuclear ribonucleoprotein A2 (hnRNPA2) and plasmid T7-driven expression 9c (pET9c)-hnRNPA2 were provided by Lexie Friend (University of Queensland, St. Lucia, Australia) (1) and Adrian R. Krainer (Cold Spring Harbor Laboratory, Cold Spring Harbor, NY) (2), respectively. pEGFP-BAG1 (B-cell lymphoma 2-associated athanogene 1) L and pEGFP–Rho-guanine nucleotide exchange factor 1 were obtained from Ann C. Williams (Bristol University, Bristol, United Kingdom) (3) and Philip B. Wedegaertner (Kimmel Cancer Institute, Philadelphia) (4), respectively. The different hnRNPA2 cDNA fragments were amplified using the pET9c-hnRNPA2 clone as a template and cloned into a plasmid entry-driven topoisomearse (pENTR-D-TOPO) vector (Life Technologies). The following primers were used to generate the PCR products comprising different fragments of hnRNPA2 (Table S1): to generate hnRNPA2 full length, PrimersAndreaOhio (PAO)-351 and PAO-338; for hnRNPA2$^{\Delta C}$-terminal region (hnRNPA2$^{\delta C}$, amino acids 1-263), PAO-351 and PAO-337; for hnRNPA2δglycine-rich domain (hnRNPA2$^{\delta GRD}$, amino acids 1–189), PAO-351 and PAO-372; for hnRNPA2glycine-rich domain (hnRNPA2^{GRD}, amino acids 190–341), PAO-374 and PAO-338; and for hnRNPA2C-terminal region (hnRNPA2^{C}, amino acids 264–341), PAO-352 and PAO-338. To generate the GST-tagged and 6xHis-tagged fragments, the pENTR-D-TOPO containing hnRNPA2 fragments was cloned into pDEST15 and pDEST17 vectors, respectively, by recombination using the Gateway LR Clonase Enzyme Mix and the conditions suggested by the manufacturer (Life Technologies). To generate the fluorescent indicator protein (FLIP) constructs, hnRNP-A2^{C} cDNA was amplified by PCR from the pET9c-hnRNPA2 vector using the PAO-379 and PAO-378 primers pair (Table S1). Fragments were cloned into the pENTR-D-TOPO vector and transferred to the 6xHis-tagged pFLIP vectors by recombination using the Gateway LR Clonase Enzyme Mix. pFLIP vectors, previously used to generate biosensors, were generously provided by Wolf Frommer (Carnegie Institution for Science, Stanford, CA) (5). The hnRNPA2^{C} fragment was cloned into pFLIP1 or pFLIP2 vectors containing the N-terminal CFP and C-terminal YFP tags or pFLIP4 vector containing the N-terminal GFP and C-terminal monomeric Kusabira-Orange. pFLIP2 and pFLIP4 vectors hold the Gateway recombination linkers flanked by the KpnI and SpeI restriction sites (Fig. S5). Different versions of FLIP2-hnRNPA2^{C} (referred as pFLIP2-1, -2-2 and -2-3-hnRNPA2^{C}) and FLIP4-hnRNPA2^{C} (referred as pFLIP4-1 and -4-2-hnRNPA2^{C}) were generated by digestion and self-ligation using KpnI and/or SpeI sites to improve FRET emission (Fig. S5).

Cell Culture. MDA-MB-231 breast cancer cells were grown in DMEM supplemented with 10% (vol/vol) FBS and 1% penicillin/streptomycin. MCF-10A immortalized breast epithelial cells were grown in DMEM/F12 medium supplemented with 10% (vol/vol) FBS, 1% penicillin/streptomycin, 20 ng/mL EGF (Prepotech), 0.5 mg/mL hydrocortisone (Sigma), 100 ng/mL cholera toxin (Sigma), and 10 μg/mL insulin (Sigma). All cells were obtained from ATCC and cultured at 37 °C in 5% CO_2 environment.

1. Friend LR, Han SP, Rothnagel JA, Smith R (2008) Differential subnuclear localisation of hnRNPs A/B is dependent on transcription and cell cycle stage. *Biochim Biophys Acta* 1783(10):1972–1980.
2. Mayeda A, Munroe SH, Cáceres JF, Krainer AR (1994) Function of conserved domains of hnRNP A1 and other hnRNP A/B proteins. *EMBO J* 13(22):5483–5495.
3. Barnes JD, et al. (2005) Nuclear BAG-1 expression inhibits apoptosis in colorectal adenoma-derived epithelial cells. *Apoptosis* 10(2):301–311.
4. Bhattacharyya R, Wedegaertner PB (2003) Characterization of G alpha 13-dependent plasma membrane recruitment of p115RhoGEF. *Biochem J* 371(Pt 3):709–720.
5. Fehr M, Frommer WB, Lalonde S (2002) Visualization of maltose uptake in living yeast cells by fluorescent nanosensors. *Proc Natl Acad Sci USA* 99(15):9846–9851.

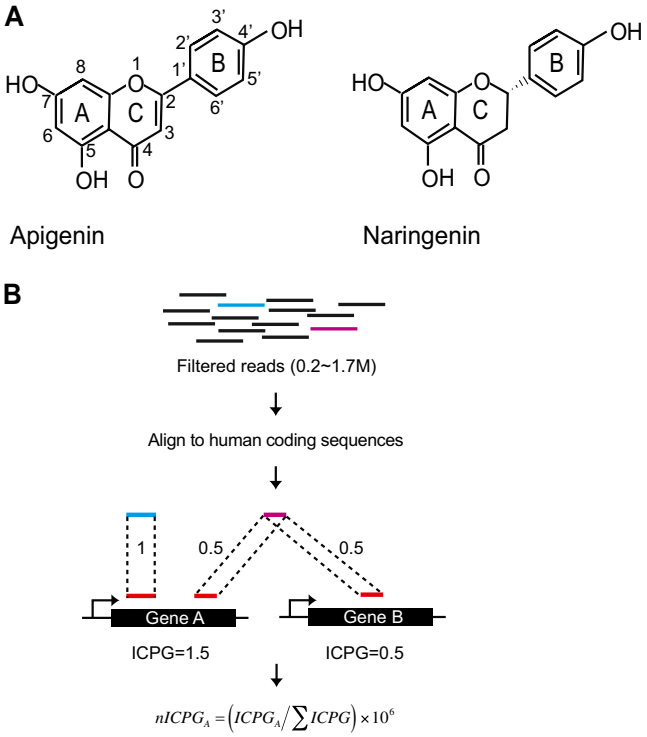

Fig. S1. Chemical structure of flavonoids and analysis of identified sequences to determine putative apigenin target enrichment. (*A*) Schematic representation of chemical structures of the flavone apigenin and the flavanone naringenin. (*B*) Calculation of normalized in frame-aligned counts per gene (nICPG) model. Sequences were filtered and aligned to human coding sequences. The number of sequences aligned in frame to a single gene was considered as the in frame-aligned count (blue bar), whereas alignment of a single sequence to multiple genes was considered as the weighted count (purple bar).

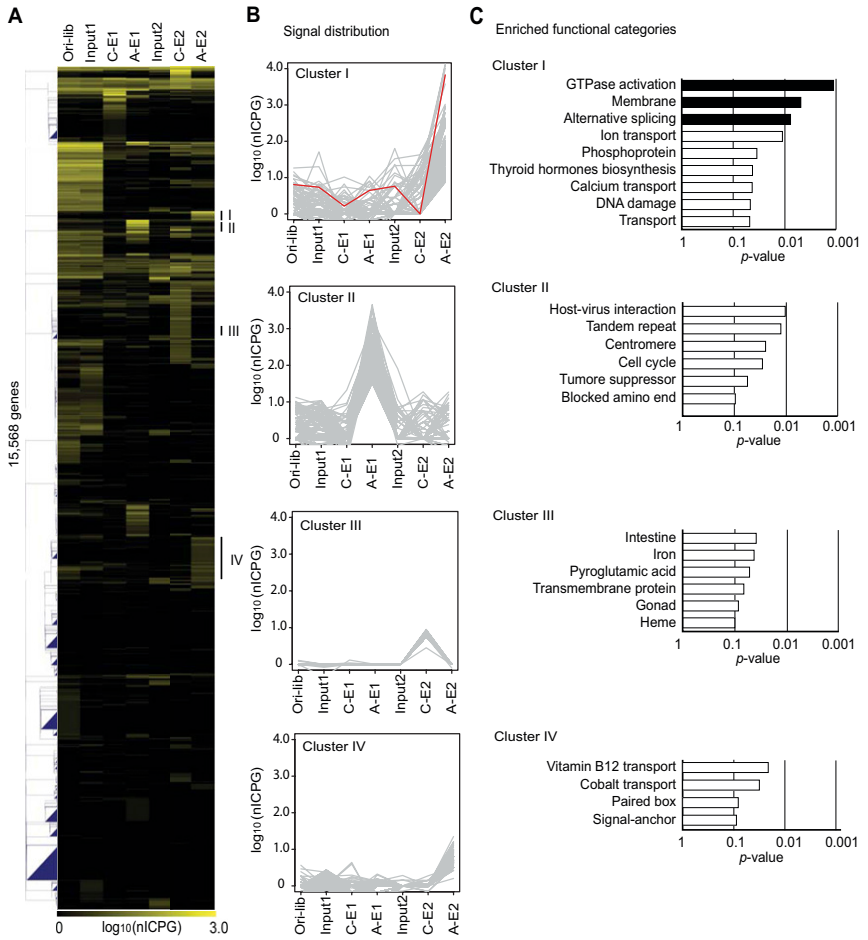

Fig. S2. Hierarchical clustering analysis of the phage display coupled with second generation sequencing (PD-Seq) results. (*A*) Heat map representation of $\log_{10}$(nICPG) for the minimal 15,568 genes present in the phage display library analyzed by hierarchical clustering using the average linkage method. The columns in the heat map correspond to the columns described in Fig. 1*C*. An enlarged view of cluster I is shown in Fig. 1*E*. Selected clusters are indicated by Roman numbers. (*B*) Line graph indicating distribution of $\log_{10}$(nICPG) within clusters. The red line indicates $\log_{10}$(nICPG) of hnRNPA2/B1. (*C*) The bar graph displays functional categories enriched in each cluster, and the *x* axis (log scale) indicates the *P* value. Filled black bars correspond to functional categories enriched significantly ($P < 0.01$).

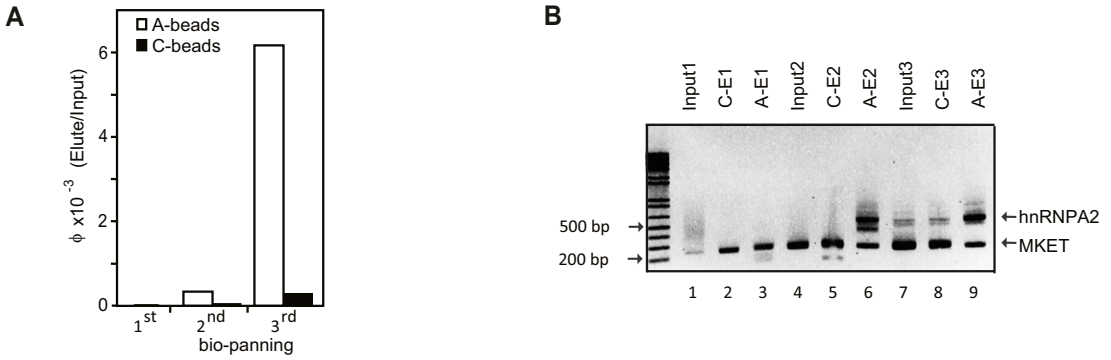

C

	Phage	Insert
A-E3-2	PNS	SGNQGGGYGGGYDNYGGGNYGSGNYNDFGNYNQQPSNYGPMKSGNFGGSRNMGGPYGGGNYGPGGSGGSGGYGGRSRY*
A-E3-5	PNS	MKETAAAKFERQHMDSPKLAAALE*
A-E3-6	PNS	SGNQGGGYGGGYDNYGGGNYGSGNYNDFGNYNQQPSNYGPMKSGNFGGSRNMGGPYGGGNYGPGGSGGSGGYGGRSRY*
A-E3-16	PNS	SGNQGGGYGGGYDNYGGGNYGSGNYNDFGNYNQQPSNYGPMKSGNFGGSRNMGGPYGGGNYGPGGSGGSGGYGGRSRY*
C-E3-1	PNS	MKETAAAKFERQHMDSPKLAAALE*
C-E3-16	PNS	MKETAAAKFERQHMDSPKLAAALE*

Red: hnRNPA2/B1

Black: MKET peptide

D

	Total reads	MCS reads*	MKET reads
Original library	4,859,548	1,014,536	2,971,167
Input1	7,817,706	1,438,079	4,640,635
C-E1	7,318,918	1,637,884	3,976,456
A-E1	5,755,257	1,231,065	2,802,825
Input2	3,863,523	769,109	2,816,430
C-E2	6,250,021	1,485,813	4,153,495
A-E2	10,694,740	1,871,830	7,407,376
Total	46,559,713	9,448,316	28,768,384

* MCS: Multicloning site (no insert)

E

DNA sequence of empty vector

Left arm — Right arm

ATG CTC GGG GAT CCG AAT TCT CCT GCA GGG ATA TCC CGG GAG CTC GTC GAC AAG CTT GCC GCG GCC GCA CTC GAG TAA

EcoRI EcoRV SmaI SacI SalI HindIII

DNA sequence of MKET clone

Left arm — Right arm

ATG CTC GGG GAT CCG AAT TCG ATG AAA GAA ACC GCT GCT GCT AAA TTC GAA CGC CAG CAC ATG GAC AGC CCA AAG CTT GCG GCC GCA CTC GAG TAA*

EcoRI HindIII

Peptide sequence of MKET clone

Left arm — Right arm

PNSMKETAAAKFERQHMDSPKLAAALE*

F

	aminoacid alingment	nucleotide alingment
MKET clone	1-MKETAAAKFERQHMDSP-17	1-ATGAAAGAAACCGCTGCTGCTAAATTCGAACGCCAGCACATGGACAGCCCA-51
Expression vector pet22-srt A	1-MKETAAAKFERQHMDSP-17	248-ATGAAAGAAACCGCTGCTGCTAAATTCGAACGCCAGCACATGGACAGCCCA-298
azorectase (Pseudomonas aeruginosa)	14-MKETAAAKFERQHMDSP-30	57-ATGAAAGAAACCGCTGCTGCTAAATTCGAACGCCAGCACATGGACAGCCCA-107
azorectase (Brevibacillus laterosporus)	18-MKETAAAKFERQHMDSP-34	41-ATGAAAGAAACCGCTGCTGCTAAATTCGAACGCCAGCACATGGACAGCCCA-91
repetitive protein BP68 (synthetic construct)	18-MKETAAAKFERQHMDSP-34	52-ATGAAAGAAACCGCTGCTGCTAAATTCGAACGCCAGCACATGGACAGCCCA-102
mutant alpha-amylase (synthetic construct)	18-MKETAAAKFERQHMDSP-34	52-ATGAAAGAAACCGCTGCTGCTAAATTCGAACGCCAGCACATGGACAGCCCA-102
kinesin tail 864 (Expression vector p864INS)	18-MKETAAAKFERQHMDSP-34	5127-ATGAAAGAAACCGCTGCTGCTAAATTCGAACGCCAGCACATGGACAGCCCA-5177
S.Tag peptide (Plasmid pPV)	6-MKETAAAKFERQHMDSP-22	1717-ATGAAAGAAACCGCTGCTGCTAAATTCGAACGCCAGCACATGGACAGCCCA-1767

Fig. S3. Conventional phage display identifies clones that bind to the apigenin-loaded beads (A-beads) and are highly enriched in the PD-Seq. (*A*) Phage (ϕ) enrichment was determined by counting pfu per milliliter in elutions from A- (white bars) and unloaded control beads (C-beads; black bars) after each round of biopanning (first, second, and third). (*B*) Enrichment of selected clones was determined by PCR using T7 primers (Table S1) flanking the insert after every round of biopanning. (*C*) Peptide sequences of apigenin binding peptides isolated by conventional phage display. Sequences in red correspond to the hnRNPA2/B1 peptide fragment, and sequences in black correspond to the MKET noncoding fragment. (*D*) Summary of sequence reads, total number of reads, multicloning site (MCS) reads, and MKET reads for each of the libraries generated and sequenced by Illumina GAII. (*E*) Nucleotide sequence of the phage MCS without insert or containing the MKET clone. (*F*) Alignment of the MKET DNA and peptide sequences indicating its probable origin.

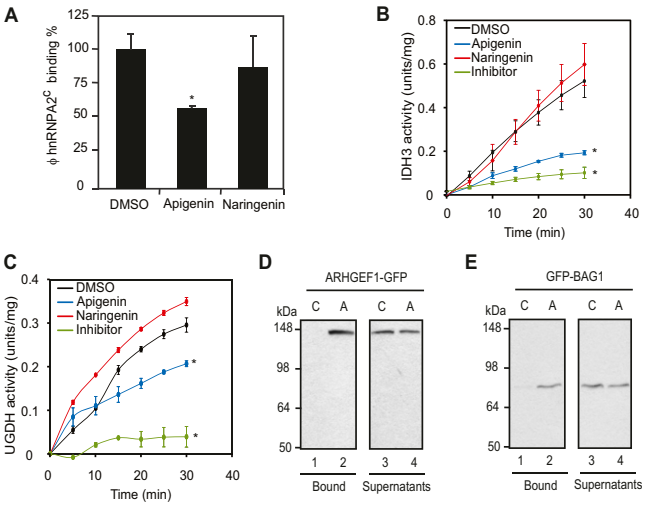

Fig. S4. Validation of apigenin targets. (*A*) A-beads were coincubated with selected phages in the presence of 20 μM apigenin, naringenin, or DMSO. Relative binding percentage to A-beads was determined by counting pfu per milliliter ϕ-hnRNPA2^{C} relative to DMSO control. Data represent the mean ± SEM ($n = 3$). *$P < 0.05$. (*B* and *C*) MDA-MB-231 cells were treated with 50 μM apigenin, naringenin, or DMSO for 3 h. (*B*) Isocitrate dehydrogenases 3 (IDH3) and (*C*) UDP-glucose dehydrogenase (UGDH) activities were measured in mitochondria and whole-cells lysates, respectively, as described in *Materials and Methods*. Iodoacetic acid (1 M), an enzymatic inhibitor, was added as control. Data represent mean ± SEM ($n = 4$). *$P < 0.05$ determined by two-way ANOVA. (*D* and *E*) Lysates from HeLa cell expressing full-length (*D*) Rho-guanine nucleotide exchange factor 1-GFP or (*E*) GFP-BCL2-associated athanogene 1 (GFP-BAG1) were used in pull-down assays with A- or C-beads (indicated as A or C, respectively), resolved by SDS/PAGE, and analyzed by Western blot using anti-GFP antibodies.

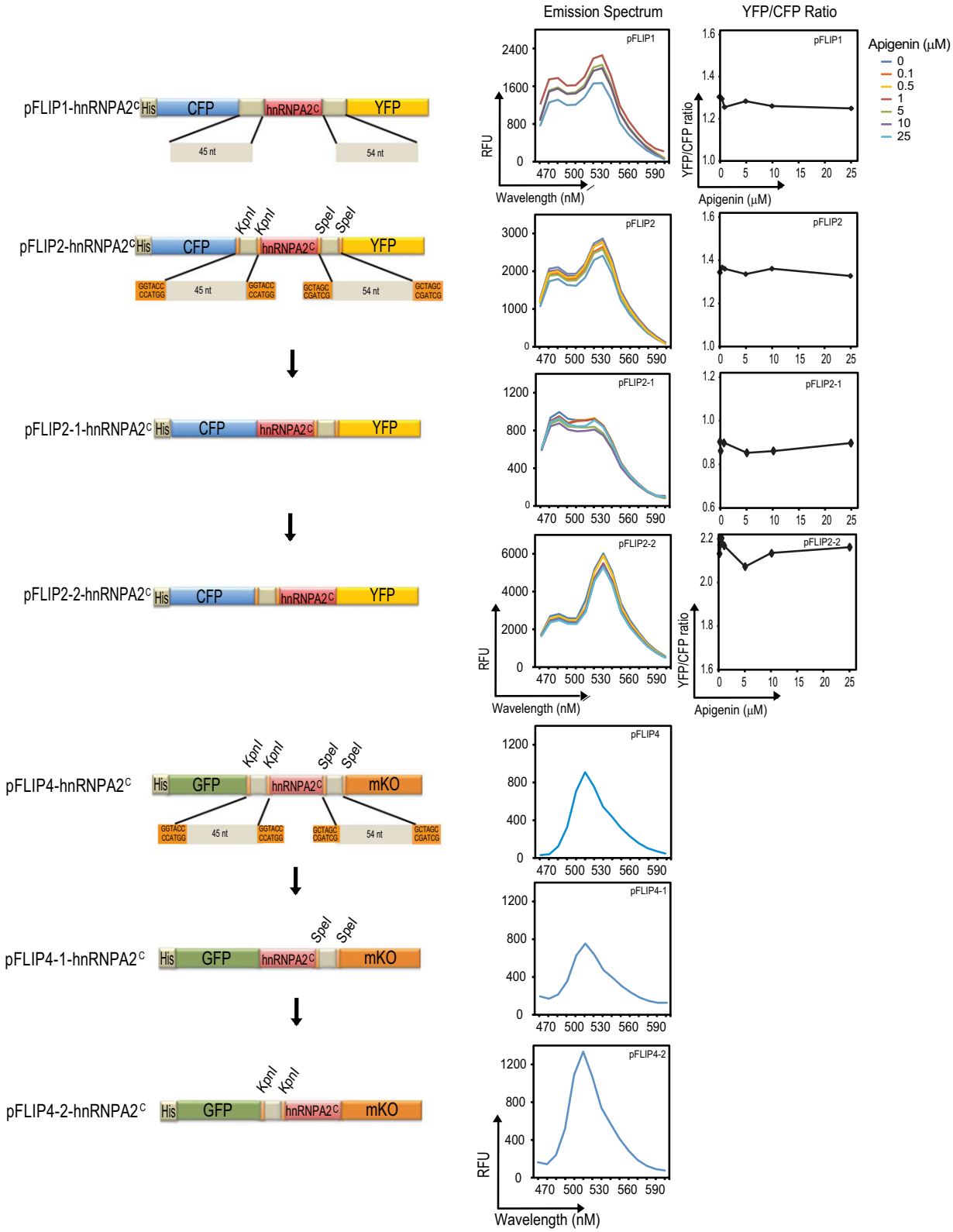

Fig. S5. Development of a flavonoid nanosensor. Bacteria lysates expressing different versions of FLIP-hnRNPA2^C proteins were incubated with increasing concentrations of apigenin (0, 0.01, 0.1, 1, 5, 10, and 25 μM) for 3 h at 37 °C. Relative fluorescence units (RFUs) were determined by spectrofluorometry (λ_{ext} = 405 nm; λ_{emi} = 460–600 nm) and represented as emission spectra. The calculated YFP/CFP fluorescent ratios (530/480 nm) are also represented over the 0- to 25-μM concentration range of apigenin.

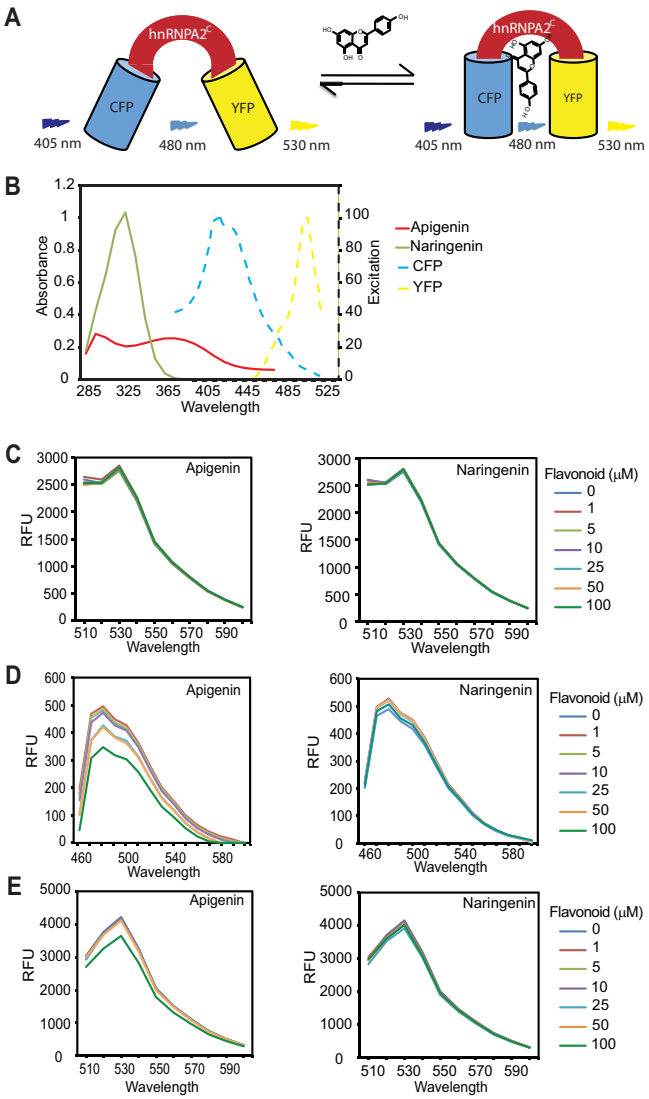

Fig. S6. Effect of flavonoids on CFP and YFP fluorescence. (*A*) Schematic representation of the flavonoid nanosensor. (*B*) Apigenin absorption spectra partially overlap with the CFP excitation spectrum. Absorption spectra of 100 μM apigenin and naringenin were measured using a spectrofluorometer plate reader over the 285- to 475-nm range. The CFP and YFP excitation wavelengths were obtained from the literature (1). (*C*) The YFP excitation/emission spectrum of FLIP-hnRNPA2^{C} was not affected by apigenin. FLIP-hnRNPA2^{C} was incubated with increasing concentrations (0, 1, 5, 10, 25, 50, and 100 μM) of apigenin or naringenin. RFUs were determined by spectrofluorometry and represented as emission spectra. (*D*) Apigenin quenches CFP fluorescence. Purified (*D*) CFP or (*E*) YFP was incubated with increasing concentrations (0, 1, 5, 10, 25, 50, and 100 μM) of apigenin or naringenin. RFUs were determined by spectrofluorometry and represented as emission spectra. CFP λ_{ext} = 405 nm; CFP λ_{emi} = 460–600 nm; YFP λ_{ext} = 475 nm; YFP λ_{emi}: 510–600 nm.

1. Patterson G, Day RN, Piston D (2001) Fluorescent protein spectra. *J Cell Sci* 114(Pt 5):837–838.

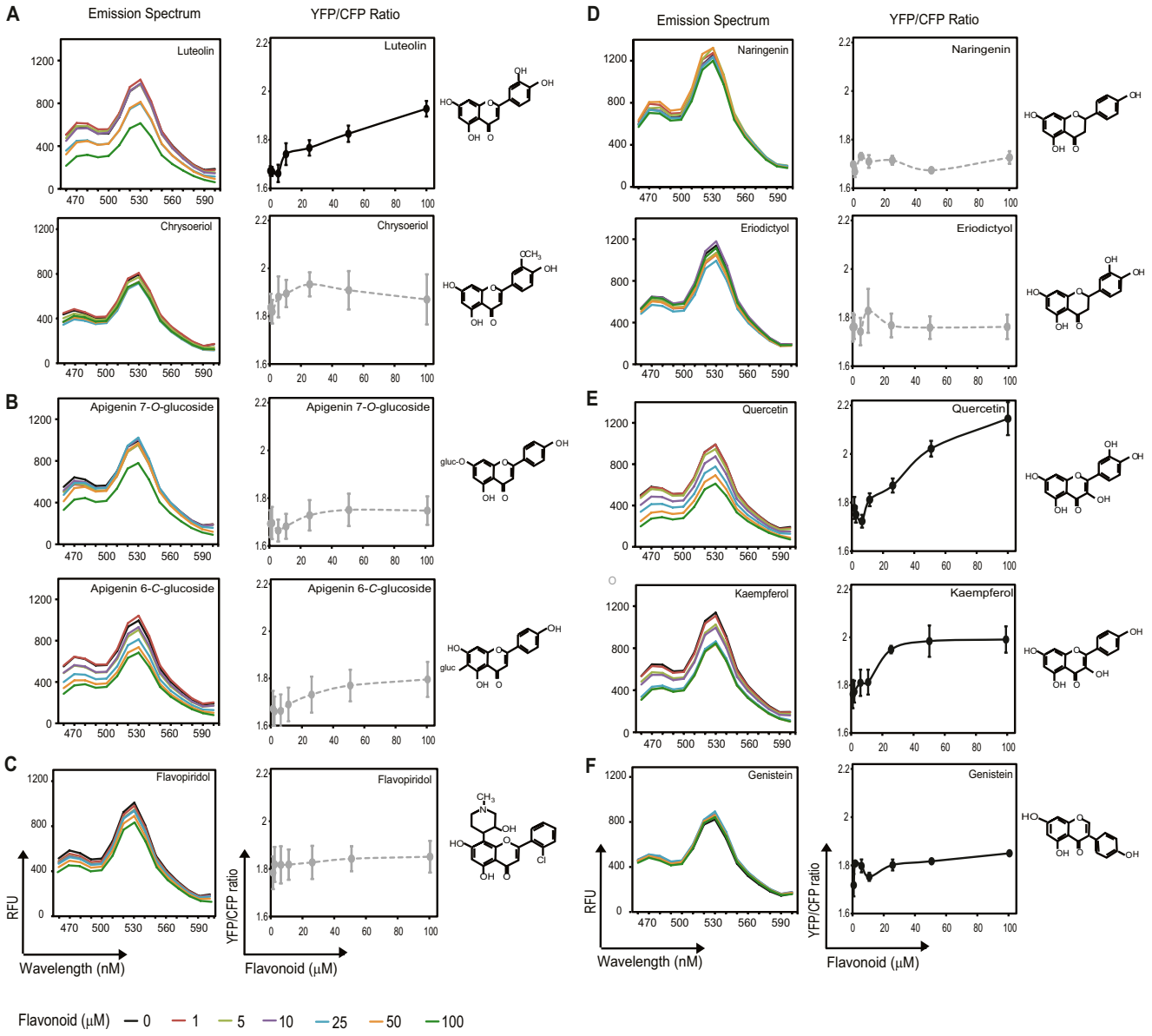

Fig. S7. Flavonoid structural relationship provided by the FRET-based flavonoid nanosensor. The affinity-purified FLIP2-3-hnRNPA2^{C} protein was incubated with increasing concentrations of the indicated flavonoids (0, 1, 5, 10, 25, 50, and 100 μM) for 3 h at 37 °C. RFUs were determined by spectrofluorometry (λ_{ext} = 405 nm; λ_{emi} = 460–600 nm) and represented as emission spectra. The calculated YFP/CFP fluorescent ratios (530/480 nm) are also represented over the 0- to 100-μM concentration range for each flavonoid. The chemical structures of the corresponding flavonoids are shown. Data represent the mean ± SEM (n = 3). (*A*) Flavones: luteolin and chrysoeriol. (*B*) Apigenin glucosides: apigenin 7-*O* glucoside and apigenin 6-*C* glucoside. (*C*) Flavopiridol. (*D*) Flavanones: naringenin and eriodictyol. (*E*) Flavonols: quercetin and kaempferol. (*F*) Genistein. Statistical significance of the variation of the observed YFP/CFP ratios over the tested flavonoid concentration range was conducted by one-way ANOVA. Black curves represent $P < 0.05$, and broken gray curves represent $P \geq 0.05$.

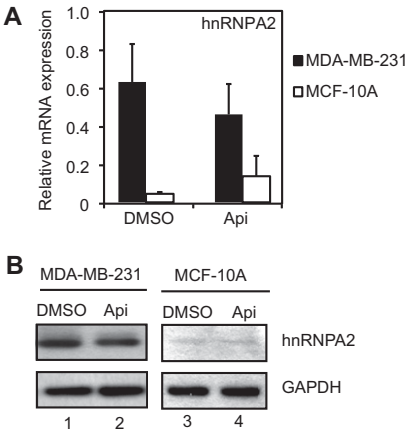

Fig. S8. Expression of hnRNPA2 in breast epithelial cells. MDA-MB-231 breast cancer epithelial cells and MCF-10A noncarcinogenic epithelial breast cells were treated with 50 μM apigenin or diluent DMSO control for 48 h. (*A*) hnRNPA2 expression was evaluated by quantitative RT-PCR. Data represents mean ± SEM ($n = 4$). (*B*) hnRNPA2 expression level determined by Western blots. Data are representative of three independent blots.

Table S1. Primers used to generate Illumina libraries, hnRNPA2 clones, and analysis of splicing

Primer	Sequence	Forward/reverse
PAO-351	5′-AAGGAAAAAAGCGGCCGCCATGGAGAGAGAAAAG-3′	Forward
PAO-338	5′-TTATAGGCGCGCCCGTATCGGCTCCTCCCA-3′	Reverse
PAO-337	5′-AAGGCGCGCCCATATCCAGGTCCTCCACCA-3′	Reverse
PAO-372	5′-AAGGCGCGCCCAGAACTCTGAACTTCCTGC-3′	Reverse
PAO-374	5′-AAGGAAAAAAGCGGCCGCCGGAAGAGGAGGCAAC-3′	Forward
PAO-352	5′-AAGGAAAAAAGCGGCCGCCGGCAACCAGGGTG-3′	Forward
PAO-377	5′-AAGGAAAAAAGCGGCCGCCGGTACCATGGAGAGAGAAAA-3′	Forward
PAO-379	5′-TTATAGGCGCGCCCACTAGTGTATCGGCTCCTC-3′	Reverse
PAO-378	5′-AAGGAAAAAAGCGGCCGCCGGTACCGGCAACCAGGGTG-3′	Forward
PAO-462	5′-AGACCAGTGGACATTGGTTC-3′	Forward
PAO-463	5′-GGTCCCTCCAGGAAACAAA-3′	Reverse
PAO-545	5′-CTTGGCCAATTTGCCTGTAT-3′	Forward
PAO-546	5′-GGCAGAAACTCTGCTGTTCC-3′	Reverse
PAO-547	5′-CGAGGCAAGATAAGCAAGGA-3′	Forward
PAO-548	5′-CACATGGAACAATTTCCAAGAA-3′	Reverse
PAO-673	5′-GGACCACCGCATCTCTACAT-3′	Forward
PAO-674	5′-TCTCCGCAGTTTCCTCAAAT-3′	Reverse
PAO-230	5′-ACTTTGGTATCGTGGAAGGACT-3′	Forward
PAO-231	5′-GTAGAGGCAGGGATGATGTTCT-3′	Reverse
T7 insert up	5′-NNNATGCTCGGGGATCCGAATT-3′	Forward
T7 insert down	5′-NNNAACCCCTCAAGACCCGTTTAG-3′	Reverse

Table S2. Summary of reads obtained by PD-Seq

Library	Total reads	Filtered reads	Aligned reads	In-frame reads
Original library	4,859,548	873,845	661,351	545,038
Input1	7,817,706	1,738,992	1,332,165	1,102,007
C-E1	7,318,918	1,704,578	1,135,646	761,372
A-E1	5,755,257	1,721,367	1,149,144	751,676
Input2	3,863,523	277,984	208,054	172,963
C-E2	6,250,021	610,713	320,373	176,654
A-E2	10,694,740	1,401,628	508,012	313,289
Total	46,559,713	8,329,107	5,314,745	3,822,999

Filtered reads correspond to the number of reads minus the MKET clone contaminant and reads with no insert (MCS reads) (Fig. S3).